Journal of Environmental Management 195 (2017) 174–185

Contents lists available at ScienceDirect

Journal of Environmental Management

journal homepage: www.elsevier.com/locate/jenvman

Research article

Iohexol degradation in wastewater and urine by UV-based Advanced Oxidation Processes (AOPs): Process modeling and by-products identification

Stefanos Giannakis [a, *], Milica Jovic [b], Natalia Gasilova [b], Miquel Pastor Gelabert [c], Simon Schindelholz [a], Jean-Marie Furbringer [d], Hubert Girault [b], César Pulgarin [a, **]

[a] SB, ISIC, Group of Advanced Oxidation Processes, École Polytechnique Fédérale de Lausanne (EPFL), Station 6, 1015 Lausanne, Switzerland
[b] Laboratoire d'Electrochimie Physique et Analytique, École Polytechnique Fédérale de Lausanne – Valais Wallis, 1951 Sion, Switzerland
[c] Escola Tècnica Superior d'Enginyeria Química (ETSEQ), Universitat Rovira i Virgili (URV), 43007 Tarragona, Spain
[d] SB, Physics Section Management, École Polytechnique Fédérale de Lausanne (EPFL), Station 3, 1015 Lausanne, Switzerland

ARTICLE INFO

Article history:
Received 12 February 2016
Received in revised form
22 June 2016
Accepted 2 July 2016
Available online 12 July 2016

Keywords:
Iodinated Contrast Media
Wastewater treatment
Urine purification
Modeling and optimization
Degradation pathway
Advanced Oxidation Process

ABSTRACT

In this work, an Iodinated Contrast Medium (ICM), Iohexol, was subjected to treatment by 3 Advanced Oxidation Processes (AOPs) (UV, UV/H_2O_2, UV/H_2O_2/Fe^{2+}). Water, wastewater and urine were spiked with Iohexol, in order to investigate the treatment efficiency of AOPs. A tri-level approach has been deployed to assess the UV-based AOPs efficacy. The treatment was heavily influenced by the UV transmittance and the organics content of the matrix, as dilution and acidification improved the degradation but iron/H_2O_2 increase only moderately. Furthermore, optimization of the treatment conditions, as well as modeling of the degradation was performed, by step-wise constructed quadratic or product models, and determination of the optimal operational regions was achieved through desirability functions. Finally, global chemical parameters (COD, TOC and UV-Vis absorbance) were followed in parallel with specific analyses to elucidate the degradation process of Iohexol by UV-based AOPs. Through HPLC/MS analysis the degradation pathway and the effects the operational parameters were monitored, thus attributing the pathways the respective modifications. The addition of iron in the UV/H_2O_2 process inflicted additional pathways beneficial for both Iohexol and organics removal from the matrix.

1. Introduction

During the last decades, research in wastewater (WW) treatment has focused on the elimination of emerging contaminants. Having efficiently tackled the classical WW issues of macropollution (organics, phosphorus, nitrogen etc), combined with the leaps in analytical chemical capabilities, micropollutants are the hottest topic in WW treatment for the last 15 years. These substances are comprising an increasing list of anthropogenic contaminants, which include among others, pharmaceuticals, personal care products, steroid hormones, industrial chemicals, pesticides and many other emerging compounds (Luo et al., 2014). The polymorphism and the diversity of the chemical pollutants, state this topic as high priority for the treatment facilities.

A distinctive category of micropollutants are the Pharmaceutically Active Compounds (PhACs), and especially the ones that are exclusively administered from hospitals. Verlicchi et al. (2012) analyzed 73 PhACs from 12 different therapeutic classes, and they concluded that most compounds are found in consistently higher concentrations in HWW than in urban WW. The antibiotics, analgesics and lipid regulators were the most concentrated, and 9 compounds posed a high risk at the concentrations detected in hospital effluent and 5 in urban WWTPs influent and effluent. Ort et al. (2010) analyzed 59 PhACs in HWW, from which 2 had a contribution higher than 15% of the total of WWTP influent. Within the "Pills-Project" (Pills project, 2012) 16 key substances out of eight substance groups in different hospitals were studied, concluding that 5 of these groups are exclusive contributors in 10–60% of the load found in urban WWTPs, and are attributed to hospital use.

* Corresponding author.
** Corresponding author.
E-mail addresses: Stefanos.Giannakis@epfl.ch (S. Giannakis), Cesar.Pulgarin@epfl.ch (C. Pulgarin).

http://dx.doi.org/10.1016/j.jenvman.2016.07.004
0301-4797/

Among these categories, the Iodinated Contrast Media (ICM) are identified as a major threat. In a recent research in a University hospital in Lausanne, Switzerland, contrast media contributed in 59% of the total PhAC load. Globally, the consumption of ICM is 35.000 tons/year (Sprehe and Geissen, 2000), from which 95% are excreted unchanged from the human body. Their use in Germany has been estimated at 500 tons of ICM per annum (Haiß and Kümmerer, 2006), while in Switzerland, the total consumption per year of ICM is estimated at 35 tons (McArdell and Kovalova, 2010). In the case of a standard Swiss University hospital, the consumption is of 1149 g/day and 725 g/day only for Iohexol (Weissbrodt et al., 2009); half of the consumed amount is rejected in HWW. This amount is reached because the individual dosage in imaging treatment is up to 300 g (Haiß and Kümmerer, 2006). ICM are non-biodegradable and only partially removed in WWTP, so their concentration in surface and drinking water is increasing, with the concentration of Iohexol in Lake Leman, Switzerland being 0.03 μg/L (Chèvre, 2014), or Iopamidol, which was found in groundwater up to 2.4 μg/L (Ternes and Hirsch, 2000).

Since the proven incapability of the existing WWTPs to handle ICM is established, their discharge to natural water bodies will contain the aforementioned amounts (Putschew et al., 2000; Ternes and Hirsch, 2000; Pérez and Barceló, 2007). Advanced Oxidation Processes (AOPs) have long been suggested as an alternative in treating non-biodegradable compounds (Pulgarin and Kiwi, 1996; Herrera et al., 1998) and many works have demonstrated the efficiency of AOPs against ICM. For example, for various ICM, such as Iopamidol, Iomeprol, Iohexol and others, very good removal was attained at basic pH with ozonation (Seitz et al., 2008), or exposure to gamma irradiation (Jeong et al., 2010), while UV/TiO_2 although it requires higher treatment times, is a treatment that can achieve high removal rates (Doll and Frimmel, 2004; Sugihara et al., 2013; Borowska et al., 2014). Nevertheless, the works that have addressed the removal in matrices as hospital wastewater or urine are scarce.

In this work, Iohexol has been chosen as a model non-ionic ICM, and has been subjected to extensive investigation concerning the various UV-based processes (UV, UV/H_2O_2, UV/H_2O_2/Fe^{2+}). In order to assess the feasibility of the treatment by UV-based AOPs, an engineering approach has firstly been made, where the investigation focuses on the matrices that Iohexol can be potentially found and measure the effect of the operational parameters in achieving 90% degradation of the initial amount in water, wastewater and urine. Also, in the view of treatment optimization by these AOPs, a modeling approach has been made for the reactants addition and pH. Finally, in order get insights on the structures affected by the different components of the process, the degradation pathway is studied for the three AOPs applied.

2. Materials and Methods

2.1. Chemicals and reagents

Table 1 presents the composition of the synthetic urine and synthetic wastewater employed in most experiments; the chemicals were used as received. Iohexol (Histodenz), hydrogen peroxide (30%) and iron sulfate heptahydrate, used for the degradation experiments, as well as KCl, Peptone, $CaCl_2 \cdot 2H_2O$ and $MgSO_4 \cdot 7H_2O$ were purchased from Sigma Aldrich (Switzerland), NaCl, Na_2SO_4, Meat Extract and NH_4Cl were acquired from Fluka (Switzerland), KH_2PO_4 and K_2HPO4 from Merck (Switzerland), while urea and creatinine from ABCR (France). Finally, titanium oxysulfate for the colorimetric determination of H_2O_2 and Ferrozine for iron detection were purchased from Fluka.

2.2. Reactors and experimental apparatus

Three “merry-go-round” reactors were used for the Iohexol degradation experiments, presented in Supplementary Fig. 1. These double coated glass vessels recirculate water at 22 °C (Neslab RTE-111 thermostat), for the protection of the UV-C equipment. UV-C light at 254 nm (5×10^{-3} mW/cm^2) was supplied to the system by low pressure (LP) mercury discharge lamps (Philips TUV 11 W/G11 T5 UV). The lamps were placed in the interior of quartz glass and then submerged in the solution inside the reactor. Mixing is ensured by a magnetic bar at the bottom of the reactor and the placement of the apparatus on a magnetic stirrer.

2.3. Analytical methods

2.3.1. Iohexol determination

The determination of Iohexol concentration was achieved through HPLC analysis (HP Agilent 1100 Series), including a G1315A diode array detector, set at 254 nm. The HPLC method was as follows: The mobile phase was held at an isocratic mode during all the analysis and consisted in the mixture of 95% ultrapure (Mili-Q) water with 0.1% of formic acid (phase A) and 5% of methanol (phase B). The flow was 1 mL/min and the temperature of the column is 40 °C and the injection volume was 50 μL. This configuration led to a retention time of 10.15 min, with a C18 reverse phase column (Merck Lichrospher 100 RP-18, 5 μm, 250–4 mm).

2.3.2. H_2O_2, Fe, COD and TOC measurements

A Shimadzu UV 1800 spectrophotometer was used for the colorimetric determination of H_2O_2 and iron. H_2O_2 was quantified by adding 10 μL of Ti(IV) oxysulfate in 1 mL of sample and subsequent measurement at 410 nm (DIN 38402H15 method). In some experiments, due to color interferences, Merck Milipore peroxide detection strips were used for semi-quantitative measurement of H_2O_2 (measurement ranges: <1.1–3 and 3–10 or <1, 1–5 and 5–10 ppm). They were employed to detect residual (<10 ppm) of H_2O_2 in real WW samples and H_2O_2 in high concentrations of Iohexol (color interference). Dissolved iron was followed with the Ferrozine method, as described elsewhere (Viollier et al., 2000). Briefly, after filtration of a 5 mL sample (0.22 μm), 0.2 mL of hydroxylamine hydrochloride, 0.2 mL of acetate buffer at pH 4.65 and 0.1 mL of 10 mM Ferrozine solution were added in the bulk. The iron determination took place by spectrophotometric measurement of the magenta color formation at 562 nm.

Pre-acquired COD (HR/LR vials, HACH Lange) were used to determine the chemical oxygen demand, and the corresponding colorimetric methods were used, measured by a HACH DR3900 Spectrophotometer. Total organic carbon and inorganic carbon of the samples during treatment were followed by a Shimadzu TOC-VCSN analyzer, with an ASI-V automatic sampling module. Finally, pH was measured with a Seven Easy pH meter (Mettler-Toledo).

2.3.3. Orbitrap MS analysis for determination of the degradation pathway

The products of Iohexol degradation were analyzed by HPLC-HR-MS. Prior to the analysis the samples were desalted using C18 SPE spin columns (Pierce Biotechnology, Rockford, IL, USA) following the manufacturer protocol. Desalted samples were separated using Dionex UltiMate 3000 UPLC system with Nucleodur C18 Gravity-SB precolumn (4 × 2 mm, 1.8 μm) and Nucleodur C18 Gravity-SB separation column (4 × 2 mm, 1.8 μm, Macherey-Nagel, Düren, Germany). The solvent A was composed of water with 0.1% FA, while solvent B contained acetonitrile with 0.1% FA. The flow rate of the mobile phase was set to 250 μL/min. The gradient consisted in the linear increase of solvent B percentage

Table 1
Synthetic matrices composition.

Synthetic urine			Synthetic wastewater		
Name	Chemical formula	SUR composition [g/L]	Name	Chemical formula	SWW composition [mg/l]
Urea	CH_4N_2O	25	Peptone	–	160
Sodium chloride	NaCl	2.925	Meat extract	–	110
Sodium sulfate	Na_2SO_4	2.25	Urea	CH_4N_2O	30
Potassium chloride	KCl	1.6	Dipotassium phosphate	HK_2PO_4	28
Potassium phosphate monobasic	KH_2PO_4	1.4	Sodium chloride	NaCl	7
Calcium chloride dihydrate	$CaCl_2{\cdot}2H_2O$	1.103	Calcium chloride dihydrate	$CaCl_2{\cdot}2H_2O$	4
Creatinine	$C_4H_7N_3O$	1.1	Magnesium Sulfate Heptahydrate	$MgSO_4{\cdot}7H_2O$	2
Ammonium chloride	NH_4Cl	1			

from 3 to 60% within 11 min. The sample injection volume was set to 35 μl. The order of events were i) column activation: MeOH/TFA 50%/0.01%, ii) column equilibration: 5% ACN 0.5% TFA, iii) sample binding: 150 μL sample, iv) washing: 5% ACN 0.5% TFA and v) elution: 80% ACN 0.1% TFA.

The MS was performed using a Q Exactive-HF-Orbitrap MS instrument (Thermo Scientific, Bremen, Germany) in positive ion mode within 200–1000 m/z. For all LC-MS runs survey scans were acquired with 15,000 resolution (at 400 m/z), automatic gain control (AGC) value of 3E6 and maximum injection time of 100 ms. Dynamic exclusion duration for the precursor ions was set to 30 s. Top 5 data-dependent MS/MS scans were recorded also with 15000 resolution (at 400 m/z), AGC value set at 1E5 and maximum injection time of 50 ms. The isolation width for the precursor ion was set to 1.8 m/z. Higher-energy collision induced dissociation (HCD) was used for the fragmentation of isolated precursor ion with normalized collision energy (NCE) of 26% and minimum signal threshold for MS/MS triggering was fixed to 20,000 counts. The obtained data were processed using Xcalibur software (3.0.63 version, Thermo Scientific, San Jose, CA, USA).

2.4. Water matrices and treatment conditions

All experiments were carried out in triplicates (3 reactors) and in different categories of matrices, i.e. water, wastewater and urine. The systematic studies took place in ultrapure water (MQ), synthetic wastewater (WW) and synthetic urine (UR). The graph data represent the average, with <5% standard deviation in the majority of cases (error bars not shown). The operational parameters tested were the following: i) Specific matrices investigated: Mili-Q water (MQ), synthetic WW, diluted synthetic WW, untreated (biologically) WW, secondary WW, synthetic urine, real urine and diluted real urine, ii) initial Iohexol concentration 10–1000 ppm, iii) initial H_2O_2 concentration 0–1000 ppm, iv) initial Fe^{2+} addition: 0–50 ppm, v) Dilution factor: undiluted, ×10 diluted, ×100 diluted and vi) starting pH: 3–11.

The composition of the synthetic WW and UR matrices was presented before. The real WW experiments involved i) the sampling from the influent and ii) the sampling after biological treatment and secondary clarification, from the WWTP of Vidy, Lausanne, Switzerland, whereas the real UR experiments succeeded the collection of urine from healthy individuals. Their main characteristics are presented in Tables 2 and 3, respectively. Finally, spiking with Iohexol to the desired level took place before each experiment.

2.5. Statistics, modeling and data treatment

For the statistical and modeling part of the investigation, the collected data were organized under separate designs of experiment. Their treatment was achieved through MINITAB software for Windows including the ANOVA and the proposed models for the k constant (first order degradation rate). The evaluation of the models is performed through the standard error (S) and the coefficient of determination (R^2).

2.5.1. Quadratic model

The model is formulated as follows:

$$\boldsymbol{k} = \boldsymbol{a}_0 + \sum_{\boldsymbol{i}} \boldsymbol{a}_{\boldsymbol{i}}\boldsymbol{x}_{\boldsymbol{i}} + \sum_{\boldsymbol{i}} \boldsymbol{a}_{\boldsymbol{ii}}\boldsymbol{x}_{\boldsymbol{i}}^2 + \sum_{\boldsymbol{i}<\boldsymbol{j}} \boldsymbol{a}_{\boldsymbol{ij}}\boldsymbol{x}_{\boldsymbol{i}}\boldsymbol{x}_{\boldsymbol{j}} \quad (1)$$

where k is the (first order) reaction constant, x_i are the model parameters and aij the respective weights.

For each experiment the first-order k constant was determined (dependent variable) and was described as a function of initial Iohexol concentration [I], H_2O_2 addition [H_2O_2], starting iron addition [Fe^{2+}] and the pH (independent variables).

2.5.2. Multiplicative model

The second model presented here is formulated as follows:

$$\boldsymbol{logk} = \boldsymbol{logc} + \boldsymbol{\gamma_i log}(\boldsymbol{x_i}) \quad (2)$$

k refers to is the reaction kinetics, x_i are the model parameters, γi

Table 2
Physicochemical characteristics of the real wastewater matrices (Margot et al., 2011, 2013; Giannakis et al., 2015).

(mg/L)	WWTP influent	Activated sludge effluent
Total suspended solids (TSS)	30	13.9
Dissolved organic carbon (DOC)	91	7.9
Chemical oxygen demand (COD)	256	30.2
Total nitrogen (in NH_4, NO_3, NO_2)	30	19.1
Total phosphorus	5.8	0.55
Alkalinity ($CaCO_3$)	n.m.	273
pH	8	7.5

n.m: not measured.

Table 3
Physicochemical characteristics of real urine matrices (own measurements and Beach, 1971).

Parameter	Low	High	Unit
TDS	24.8	37.1	g/L
pH	6.2	8.3	
COD	6.1	10.6	g/L
TKN	4.8	7.9	g/L
TOC	3.6	6.7	g/L
Average			
Inorganic salts	14.2		g/L
Urea	13.4		g/L
Organic compounds	5.37		g/L
Organic ammonium salts	4.1		g/L
Total solutes	37.1		g/L

the corresponding weight, while c is a numerical constant.

Given that all the parameters can be expressed in logarithmic terms (as concentrations), the model can be written as above. The independent variables assume 0.01 instead of 0 in the Iohexol, H_2O_2 and Fe^{2+} concentrations, and the pH of the solution is expressed as $-\log[H^+]$. Therefore, the Equation (2) is expressed as follows:

$$\boldsymbol{\log k = \log c + \gamma_i \log(x_i) \rightarrow k = c \prod_{i=1}^{n} x_i^{y_i}} \quad (3)$$

With the aforementioned transformation, the model takes a rather simple form of a product between the independent variables, directly connected with the reaction constant k.

3. Results and discussion

3.1. Engineering approach – investigation on the operational parameters

3.1.1. Iohexol, H_2O_2 and water matrix effect on $t_{90\%}$

In the first part of this study, the operational parameters involved in the UV/H_2O_2 AOP process were investigated, namely the concentration of Iohexol, the addition of H_2O_2 and the matrix containing the contaminant. Fig. 1 depicts the influence of concentration of the drug (I) and the oxidant (H_2O_2), in Mili-Q (MQ) water. As it has been previously reported (Pereira et al., 2007), Iohexol is rather susceptible to UV treatment alone. The high molar absorption coefficient of Iohexol at 240 nm (Borowska et al., 2014) makes the treatment by the high energetic UV-C photons effective. According to the level of drug addition, the time necessary to degrade the pollutant starts from a matter of minutes (10 ppm) and exceeds 10 h (1000 ppm) for this relatively low light intensity used in our experiments. The good linear profile of the fitted lines in log Y scale ($R^2 > 99\%$) indicate that the degradation follows pseudo first order kinetics. The threshold of 90% degradation is set to ensure elimination of the compound and offer a ground of comparison among the various processes that will follow, which is calculated as $t_{90\%} = -(\ln 0.1)/k$.

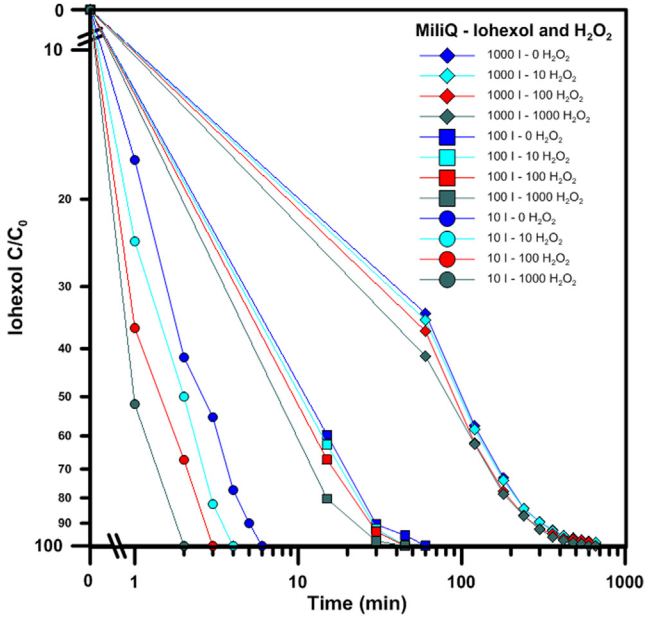

Fig. 1. UV photolysis and UV/H_2O_2 experiments in Mili-Q water. Note that the results in the 10–1000 mg/L range are plotted in double-logarithmic scale and axis breaks for clarity purposes only.

In the former experiment, H_2O_2 was also added in a log-stepwise manner. The homolytic disruption of the HO–OH bond results in the release of the second most powerful oxidant, the hydroxyl radical (HO•) (Guo et al., 2013). In the past, adding small quantities of H_2O_2, when LP UV was used, has not sufficiently improved the degradation of Iohexol in water matrices (Pereira et al., 2007; De la Cruz et al., 2012, 2013), but the concentrations never exceeded the "economic" range. Here, we reached up to 1000 ppm H_2O_2 initial addition, and the results are presented in the different color traces of Fig. 1. Iohexol is mostly affected by the hydroxyl radical addition to the aromatic ring, as hydrogen abstraction or electron transfer are either slower or less common pathways (Zhao et al., 2014). Nevertheless, it appears that the process is mildly affected in its totality, since the $t_{90\%}$ is moderately improved. Also, since the first order models also fit well this process, we can corroborate with previous findings (Sharpless and Linden, 2001; Pereira et al., 2007) that most probably, the efficiency of direct photolysis is very high.

Similar investigation also took place in (synthetic) wastewater (WW) and (synthetic) urine (UR) matrices. These matrices represent the main conditions in which Iohexol is encountered, and the effect of the matrix is here investigated. Table 4 summarizes the $t_{90\%}$ calculated in the different experiments, varying the initial Iohexol and H_2O_2 amount, as a first step. A marginal improvement is observed as the ratio of Iohexol/H_2O_2 is modified, as found in the MQ matrix before. However, although $t_{90\%}$ times for WW remained close to the observed ones for MQ, synthetic urine values did not drop significantly for low (10 ppm) Iohexol content, but were rather similar to the 100 ppm ones. The explanation lies in the competition for the HO• radicals generated by the process. In wastewater, the oxidizable organic and inorganic components are significantly less than in urine, which makes the degradation of mg/L quantities easier. Normally, for compounds that are highly photo-oxidized, the effect of the organic matter is usually not very profound (Canonica et al., 2008). Hence, a parameter which could greatly affect the application of the process and would need further investigation is the possible dilution of the concentrated WW and UR, and then treatment with AOPs.

3.1.2. Effect of matrix dilution and Fenton-initiated enhancement of the process on $t_{90\%}$

Fig. 2 showcases the wastewater and urine experiments plus the comparison between undiluted and diluted (×10 times) matrix, while featuring the addition of Fe^{2+} in the system and the drop of the pH up to 3.

For WW (Fig. 2a), dilution had an effect on the degradation

Table 4
$t_{90\%}$ evolution (min) in varied Iohexol (10–1000 ppm) and H_2O_2 (0–1000) levels.

	$t_{90\%}$	Iohexol/H_2O_2			
		1000/0	1000/10	1000/100	1000/1000
Matrix	*MQ*	324	320	311	268
	WW	371	360	329	291
	UR	535	523	501	461
		100/0	**100/10**	**100/100**	**100/1000**
Matrix	*MQ*	33	28	26	19
	WW	35	29	27	22
	UR	204	184	141	122
		10/0	**10/10**	**10/100**	**10/1000**
Matrix	*MQ*	7	5	4	3
	WW	10	7	6	3
	UR	168	154	139	122

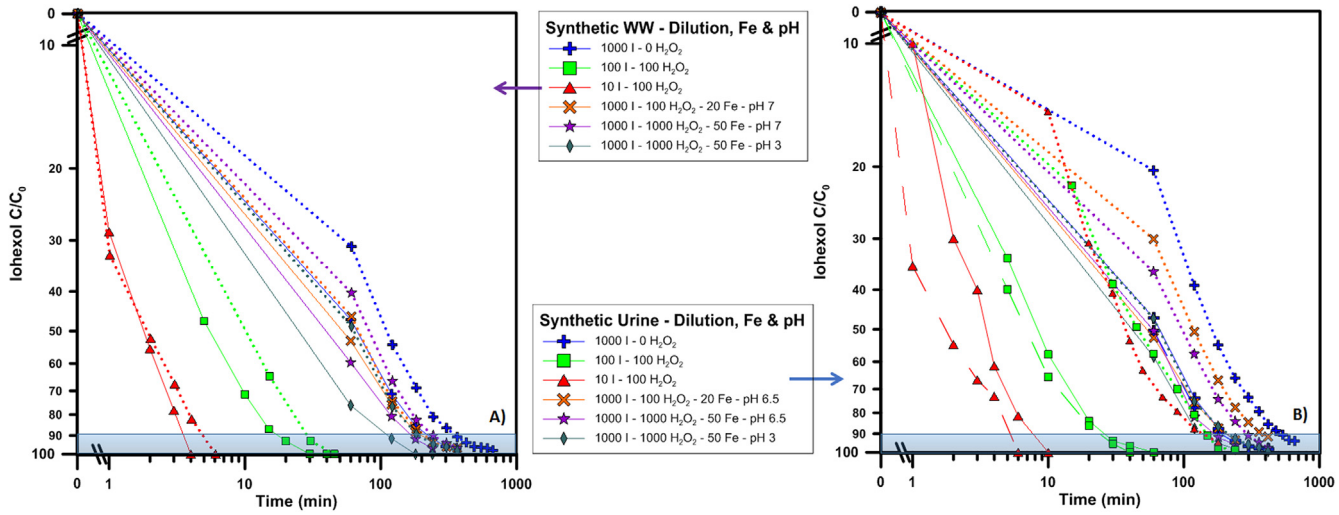

Fig. 2. Effect of pH, dilution and Iohexol, H_2O_2 and Fe^{2+} amounts. Dotted lines represent the undiluted matrices, continuous lines indicate the ×10 times dilution experiments, and for Fig. 3b, the ×100 times diluted UR experiments are signified with long dashed lines. Note the mixed axes scales.

efficiency, decreasing as the initial Iohexol content is decreasing. The diluted matrix now presents less competition for the HO•, effectively targeting the contaminant. However, for the same reason, milder effect on the addition of iron now occurs, as, along with the antagonistic nature, the synergistic metal complexing effects of the organic matter, leading to a higher Fe^{3+} solubility and consequently a more efficient Fenton and photo-Fenton cycle, are now mitigated. Nevertheless, the dilution plays an important role and ~20% improvement in degradation is measured. This suggests confidently that reducing the organic matter of the water, for instance with an activated sludge process could enhance the efficiency of the downstream UV/H_2O_2/Fe^{2+} AOP applied, the participation of the matrix, but also the recalcitrance of the compound while treated, since the improvement is not impressive.

Furthermore, in Fig. 2b we observe a similar improvement in UR treatment when ×10 dilution is applied in the system. In average, the improvement is higher than the respective one in WW, with almost ~40% minimum increase in the efficiency. The new matrix composition absorbs less UV inefficiently (nitro-, amino- and phosphoric compounds from the synthetic recipe), thus efficiently targeting Iohexol, and also the generated radicals target the contaminant without being overly wasted. Technically, using a secondary water from other sources in a hospital could be feasible; for example water from deionization units, or even greywater (having considerably lower organic and inorganic content than urine) could be used for the dilution. Of course, hydraulic optimization of the reactor and construction costs will play an important role, which is beyond the scope of this research.

3.1.3. Experiments in real wastewater and urine matrices

3.1.3.1. Real wastewater. In municipal wastewater, we tested the lower two concentrations assayed in the synthetic matrix, before and after secondary treatment of the WW inflow, varying the Iohexol spiking, the H_2O_2/Fe^{2+} addition levels and the pH in the beginning of the experiment.

Fig. 3a suggests that, as a rule of thumb, acidification increased efficiency and moving towards the natural pH, the removal is hampered. The initial physicochemical conditions differ significantly among the two matrices with suspended solids, which block light transmission, being double before treatment. Secondly, the organic content removed in the activated sludge unit greatly benefited the process demonstrating 50% reduction in the removal of Iohexol (10 ppm) and almost 20% in the 100 ppm experiments. The reduction of the organics content permitted the redirection of the HO• radicals against the contaminant, which is less effective when high amounts of Iohexol were added.

However, the degradation in WW is a complex system, with various forces which aid or act antagonistically either to the photolysis or the production of hydroxyl radicals. Other parameters that influence the efficiency are the nitrogen, phosphorus and carbonate-related compounds. Nitrate exposed to UVC at 254 nm has been shown to undergo photo-transformations. With the participation of peroxynitrite and peroxinitrous acid, either nitric acid or nitrite is produced (Mack and Bolton, 1999). The nitrite, reacts with the hydroxyl radicals, producing nitrite radicals (Vione et al., 2014). Phosphorus on the other hand consumes hydroxyl radicals, and also precipitates by the iron salts, which actively reduces the available iron for the complementary photo-Fenton action. Finally, (bi)carbonates are known not only to scavenge the hydroxyl radicals, but also to form the carbonate radicals, which have mild oxidative action (Wu and Linden, 2010).

3.1.3.2. Real urine. For the experiments involving real urine, the initial COD values ranged between 2.8 and 9.5 g/L and DOC 2.5–7 g/L, corroborating with the literature suggesting similar values, previously presented in Table 3. Treatment Iohexol in urine (Fig. 3b) revealed only two different families of graphs, i.e. the diluted and undiluted urine experiments. Firstly, pH modification and the addition of the Fenton reagents did not enhance significantly the degradation rate. The vertical bars indicating the improvement are smaller than the respective wastewater ones. Secondly, when treating Iohexol in undiluted urine, almost regardless of the method or reactant addition, both 100 and 1000 ppm experiments required a significantly elevated time to complete. Apart from the suspended solids, the reactants involved in wastewater, concerning nitro-, phosphoro- and carbonate-compounds here are in higher amounts, compared to wastewater, and the implications are expected to make the degradation scheme more complex.

Also, urine contains large amounts of proteins, such as urobilin, serum albumins, transferrins etc, some of which contain groups which absorb in the UV region. On the other hand, transferrins can bind the iron (Davis et al., 1962), which limit the participation in the Fenton reaction (Papoutsakis et al., 2015a). This hypothesis is

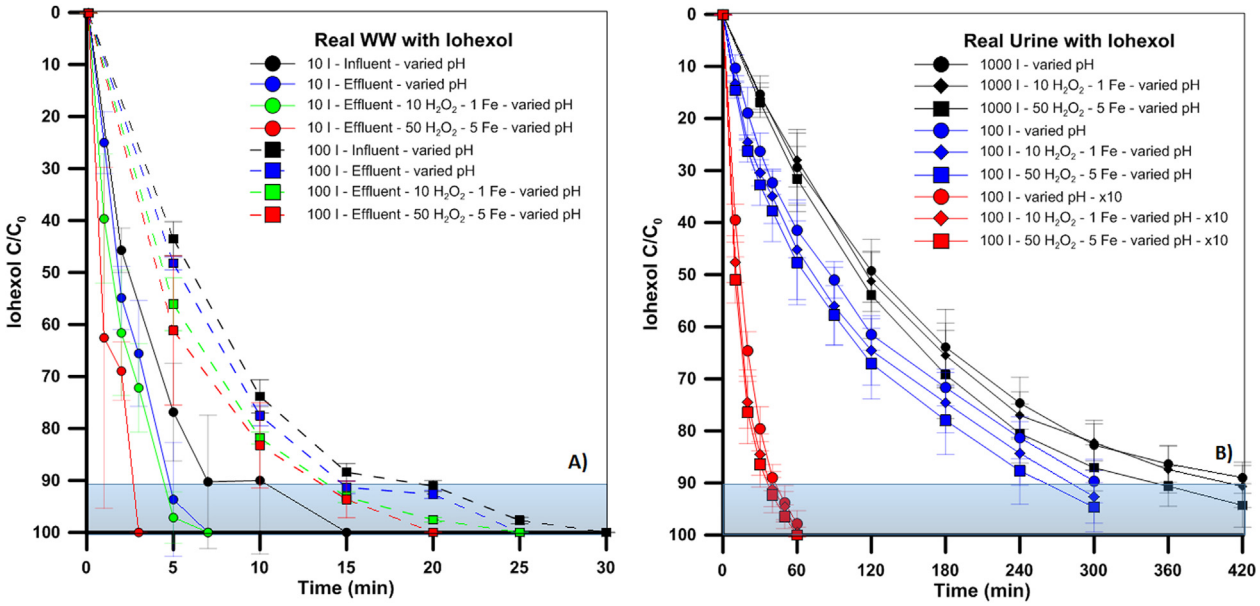

Fig. 3. Real wastewater and urine experiments: UV/H_2O_2/Fe^{2+} process. A) Iohexol in untreated or biologically treated WW, and B) diluted/undiluted urine, H_2O_2 added in 0, 10 or 50 ppm, iron was added in 0, 1, or 5 ppm, and changing of the initial pH value (3, 5 or near-neutral). The two main groups of Fig. 3a data are separated by continuous (10 ppm Iohexol) or dashed lines (100 ppm). The respective groups in Fig. 3b are designated by color. The vertical bars show the variation in efficiency when pH was changed. Note the mixed axes scales.

further strengthened when examining the diluted urine matrix. If ×10 dilution is applied, the need to acidify and add the Fenton reactants is lower, as they marginally contribute to the degradation. Although a bigger reactor theoretically would be necessary, the economical and operational costs are considerably lower than the ones necessary for improving the process in undiluted urine.

3.2. Statistical approach – modeling and mathematical optimization of the treatment

A general finding of the previous part was that there were no significant differences between the results found in synthetic and real WW and UR matrices, therefore the laboratory tests can be extrapolated in the real context. Also, it means that in two different matrices, we could predict the time necessary for degradation ($t_{90\%}$), based only on broad indications about the target matrix and the order of magnitude of Iohexol concentration. For the aforementioned reasons, we attempt to model the degradation process (first order degradation constant k), based on the laboratory experiments already presented in the previous chapter.

The models, to which the data will be fitted, have been presented in the Materials and Methods section. For identifying the coefficients of these models, we have completed the experiments presented in the previous section with additional experimental points, to constitute a Central Composite Design (CCD), which summary is as follows:

- Iohexol was kept constant, at 100 mg/L.
- H_2O_2 and Fe^{2+} values were kept in a low amounts, in all matrices.
- pH was tested among 3 and 5 (to better take advantage of the conditions that favor the Fenton reaction).

Table S1 of the Supporting Information presents the data points and the levels of the parameters used in the CCD. The experiments added from the previous section bring different Iohexol and Fenton reagent amounts, as well as alternative pH values (near neutral and basic, only for WW).

As a general strategy for both matrices, a step-wise construction of the model took place, as follows: After removal of the outliers and through regression, different models were fitted. Their expressions are presented in Table 5 for WW and Table 6 for UR. For the multiplicative model, the logarithmic values of the various levels and the response variable k were used; we remind that for pH, its definition of the −log [H^+] was used.

Two evaluation criteria have been used, i.e. the standard error (S) and the coefficient of determination (R^2, %). ANOVA was also performed (the detailed ANOVA tables can be found in the Supplementary material) and put in evidence the order of importance among the factors.

Iohexol > H_2O_2 or pH > Fe^{2+}

This order is only qualitative since often the Fenton reagents and the pH failed to pass the P-test of 95% confidence interval (e.g. Table S1.1.1 or Table S1.1.5. in Supplementary Material). Also, the order among H_2O_2 and pH depends on the matrix, with WW regarding the H_2O_2 addition as most important and UR matrices (especially the undiluted) depending more on the pH. This effect can be attributed to the efficient photolysis or the homolysis of H_2O_2 in the more transparent matrices, compared to UR, whereas acidification favors the photo-Fenton participation.

As it is clearly shown in the two previous Tables 5 and 6, the process cannot be described fairly by a linear model. The interactions and/or the square terms need to be added. In all cases, Iohexol amount is the most important factor in determining the order of magnitude of the k constant. The use of the multiplicative model provides a far simpler expression, without conceding much in terms of accuracy in most of the cases. As the scale is different, the importance of the parameters is also changed, with pH becoming more important for wastewater and Fe^{2+} for urine.

The prediction of degradation time holds high importance for the technical applications, therefore optimization of the models has been assayed. The problem is broken down to maximizing an objective function k = f (Iohexol, H_2O_2, Fe^{2+}, pH). The optimization took place through the desirability function (Harrington, 1980;

Table 5
Wastewater models with S and R^2 values.

Wastewater	Linear	Linear w/squares	Quadratic	Wastewater	Multiplicative
Linear				**Linear**	
Constant	1.46E-01	3.56E-01	3.36E-01	Constant	9.33E-01
[I]	−1.43E-04	−2.86E-03	2.85E-03	log[I]	−9.75E-01
$[H_2O_2]$	2.30E-05	2.93E-04	3.33E-04	log$[H_2O_2]$	2.79E-02
$[Fe^{2+}]$	−8.00E-05	2.89E-03	5.08E-03	log$[Fe^{2+}]$	1.07E-01
pH	−1.69E-03	−3.14E-03	−3.00E-04	log$[H^+]$	2.32E-02
Squares					
[I] × [I]		3.00E-06	3.00E-06		
$[H_2O_2]$ × $[H_2O_2]$		−1.00E-06	1.00E-06		
$[Fe^{2+}]$ × $[Fe^{2+}]$		−6.10E-05	−1.20E-04		
pH × pH		−7.30E-05	−1.97E-04		
Interactions					
[I] × $[H_2O_2]$			−1.00E-06		
[I] × $[Fe^{2+}]$			−2.00E-06		
[I] × pH			−5.00E-06		
$[H_2O_2]$ × $[Fe^{2+}]$			3.00E-06		
$[H_2O_2]$ × pH			1.20E-05		
$[Fe^{2+}]$ × pH			−1.01E-04		
S	0.07	0.02	0.02	S	0.10
R^2	38.44	92.38	93.90	R^2	96.62
Diluted wastewater	Linear	Linear w/squares	Quadratic	Diluted wastewater	Multiplicative
Linear				**Linear**	
Constant	2.48E-01	6.68E-01	6.29E-01	Constant	1.37E+00
[I]	−2.39E-04	−3.33E-03	−3.79E-03	log[I]	−9.18E-01
$[H_2O_2]$	9.80E-05	8.70E-05	2.69E-04	log$[H_2O_2]$	5.60E-03
$[Fe^{2+}]$	−1.74E-03	1.50E-03	1.11E-02	log$[Fe^{2+}]$	6.56E-02
pH	3.00E-04	−8.45E-02	−7.70E-02	log$[H^+]$	8.60E-02
Squares					
[I] × [I]		3.00E-06	3.00E-06		
$[H_2O_2]$ × $[H_2O_2]$		−1.00E-06	2.00E-06		
$[Fe^{2+}]$ × $[Fe^{2+}]$		4.10E-05	−1.08E-04		
pH × pH		7.69E-03	7.00E-03		
Interactions					
[I] × $[H_2O_2]$			−1.00E-06		
[I] × $[Fe^{2+}]$			−2.00E-06		
[I] × pH			1.70E-05		
$[H_2O_2]$ × $[Fe^{2+}]$			−3.00E-05		
$[H_2O_2]$ × pH			2.00E-05		
$[Fe^{2+}]$ × pH			−6.30E-04		
S	0.08	0.04	0.04	S	0.17
R^2	61.38	92.50	95.76	R^2	92.24

Papoutsakis et al., 2015b). This method allows the simultaneous optimization of several equations. The desirability function for each equation is given by the following expression (Equation (4)):

$$d = \begin{cases} 0, \text{ for } y \le y_{min} \\ \left(\dfrac{y - y_{min}}{y_{max} - y_{min}}\right)^{W_i}, \text{ for } \quad y_{min} < y < y_{max} \\ 1, \text{ for } y \ge y_{max} \end{cases} \tag{4}$$

Since normalization of the parameters has taken place, the R different desirability functions d can be combined to the (overall) desirability function, for the k constant, as follows (Equation (5)):

$$D = \left(\prod_{r=1}^{R} d_r\right)^{\frac{1}{R}} \tag{5}$$

- R is the number of functions,
- d the desirability of each function and
- D the desirability of the system.

The optimization results are presented in Table 7, showing the desirability function values and the operating regions. As it appears, the optimal region for maximizing the k constant is when Iohexol is minimal, as the addition of higher amounts of Iohexol changes dramatically the k values. As expected, for the linear models we found the optimum at the border of the experimental domain.

For the quadratic model in the undiluted matrices, the gains from the increase of the Fe^{2+} amounts starts to get mitigated and values around 20–30 ppm are suggested. This is probably caused by the physical blocking of UV light by the iron particles. Between WW and UR, the difference is found in the Fe^{2+} amount added, as more iron is suggested in the case of WW. Since in UR acidification of the matrix was recommended, less iron was suggested for the optimal performance in this case. As far as the desirability of the proposed operating regions is concerned, the linear models did not produce solutions very close to D = 1. On the other hand, the quadratic models often found the optimal regions and the desirability of the system is ~1.

In conclusion, our statistical approach resulted in models with satisfactory performance (based on S and R^2 values). However, the optimization with a single response variable is relatively blindsided by other factors, such as the cost of the process. In that case, the optimal region would be a compromise among the efficiency and the cost. It is recommended that the quadratic model has to be preferred but in further work, more response variables should be taken into consideration, such as involving the cost of reagents, iron

Table 6
Urine models with S and R^2 values.

Urine	Linear	Linear w/squares	Quadratic	Urine	Multiplicative
Linear				**Linear**	
Constant	9.28E-02	1.86E-01	1.02E-01	Constant	−3.39E-01
[I]	−2.50E-05	8.90E-05	−2.30E-04	log[I]	−3.37E-01
$[H_2O_2]$	−9.00E-05	−1.22E-04	−2.47E-04	log$[H_2O_2]$	7.90E-03
$[Fe^{2+}]$	2.38E-04	2.47E-03	9.33E-03	log$[Fe^{2+}]$	2.20E-01
pH	−1.02E-02	−6.29E-02	−2.06E-02	log$[H^+]$	1.33E-01
Squares					
[I] × [I]		−1.00E-06	1.00E-06		
$[H_2O_2] \times [H_2O_2]$		1.00E-06	−1.00E-06		
$[Fe^{2+}] \times [Fe^{2+}]$		−5.00E-05	−1.41E-04		
pH × pH		5.56E-03	1.12E-03		
Interactions					
$[I] \times [H_2O_2]$			−1.00E-06		
$[I] \times [Fe^{2+}]$			2.00E-06		
[I] × pH			2.90E-05		
$[H_2O_2] \times [Fe^{2+}]$			5.00E-06		
$[H_2O_2]$ × pH			4.20E-05		
$[Fe^{2+}]$ × pH			−1.25E-03		
S	0.02	0.01	0.01	S	0.17
R^2	59.52	79.59	95.81	R^2	83.42
Diluted urine	**Linear**	**Linear w/squares**	**Quadratic**	**Diluted urine**	**Multiplicative**
Linear				**Linear**	
Constant	1.19E-01	2.41E-01	2.30E-01	Constant	2.08E-01
[I]	−1.60E-04	−1.31E-03	−1.05E-03	log[I]	−6.35E-01
$[H_2O_2]$	6.14E-04	9.10E-05	−1.63E-04	log$[H_2O_2]$	5.05E-02
$[Fe^{2+}]$	−1.33E-03	−8.40E-04	−5.40E-04	log$[Fe^{2+}]$	1.43E-01
pH	2.33E-03	−1.10E-03	−5.50E-03	log$[H^+]$	3.39E-02
Squares					
[I] × [I]		1.00E-06	1.00E-06		
$[H_2O_2] \times [H_2O_2]$		3.00E-06	2.00E-05		
$[Fe^{2+}] \times [Fe^{2+}]$		4.70E-05	6.20E-05		
pH × pH		−7.70E-04	4.00E-04		
Interactions					
$[I] \times [H_2O_2]$			−1.00E-06		
$[I] \times [Fe^{2+}]$			–		
[I] × pH			–		
$[H_2O_2] \times [Fe^{2+}]$			−4.00E-06		
$[H_2O_2]$ × pH			1.10E-04		
$[Fe^{2+}]$ × pH			−1.54E-04		
S	0.03	0.01	0.01	S	0.08
R^2	76.14	95.08	95.39	R^2	95.39

reclamation, residual H_2O_2 elimination, pH neutralization and others as in other works (e.g. Papoutsakis et al., 2015b).

3.3. Analytical approach — global measurements (COD, TOC, and UV-vis absorbance) combined with specific HPLC and MS analysis

The combination of the findings of the previous two parts do not fully support the idea of using H_2O_2 to enhance the degradation efficiency of Iohexol in aqueous matrices. Therefore in this part, an effort has been made to decode the reasons behind this effect and propose the proper operational conditions under a new prism.

In Fig. 4(a–d) we present the profiles of the transformation products (TPs) by Peaks (area) vs. time graphs. The operational conditions were set to Iohexol at 1000 ppm and H_2O_2 logarithmically increasing from 0 (UV photolysis) to 1000 ppm (highly oxidative conditions). In all figures, the treatment was stopped after 11 h and the colored lines of the graphs represent the TPs by their elution time, corresponding to Iohexol and the generated by-products under the different studied conditions. We have excluded the peaks below 3.5 min elution time as they represent highly-polar aliphatic acids, with low absorbance and non-linear correspondence to the UV detector set at 254 nm. Also, a representative chromatogram can be found at the supplementary material (Fig. S2).

As it can be observed, the degradation of the parent compound is proceeding in all cases as time progresses (peak at 10.12 min)

Table 7
Optimal regions for treatment Iohexol through optimization by the desirability function.

Wastewater	Iohexol	H_2O_2	Fe^{2+}	pH	D	Urine	Iohexol	H_2O_2	Fe^{2+}	pH	D
Linear	10	1000	50	lowest	0.3947	Linear	10	1000	50	lowest	0.7815
Quadratic	10	1000	32.3	7	1	Quadratic	10	1000	22.7	lowest	1
Diluted WW	Iohexol	H_2O_2	Fe^{2+}	pH	D	Diluted UR	Iohexol	H_2O_2	Fe^{2+}	pH	D
Linear	10	1000	50	lowest	0.7401	Linear	10	1000	50	7	0.7829
Quadratic	10	1000	1	7	1	Quadratic	10	1000	1	7	0.9986

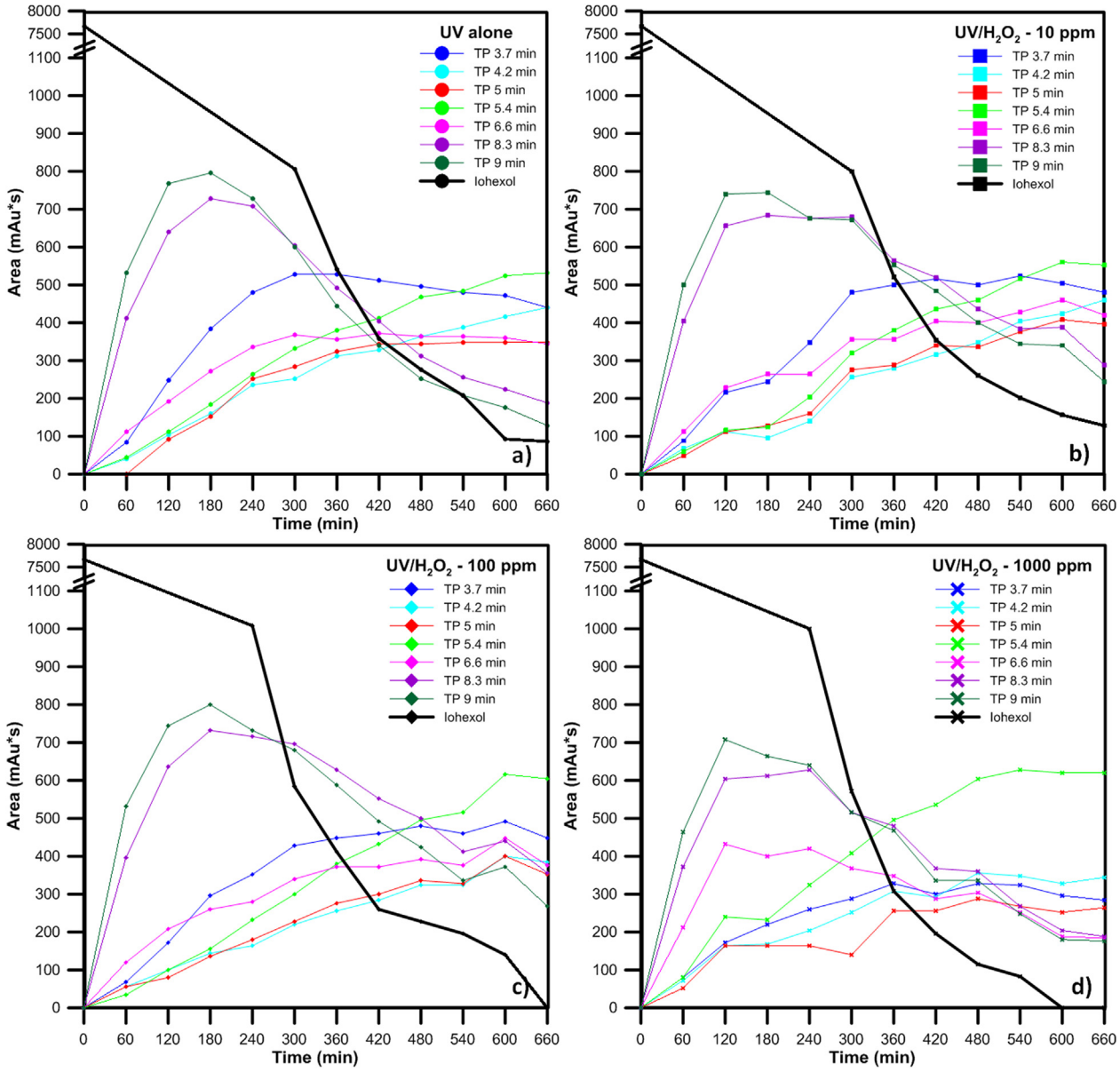

Fig. 4. HPLC peak areas evolution during Iohexol degradation by the UV photolytic and photocatalytic process. A) UV only, B) 10 ppm H_2O_2, C) 100 ppm H_2O_2, D) 1000 ppm H_2O_2. 100 ppm of Iohexol was chosen as initial spiking.

towards complete elimination, but achieved only when 100 and 1000 ppm H_2O_2 were used. During the degradation of Iohexol, intermediate peaks appear in distinctive times, representing the more polar by-products resulting from the elimination of Iodine atoms, the −OH addition and the side chains breakage from the central aromatic ring. Also, it can be observed that increasing the H_2O_2 concentration also leads to faster peak maxima in mid-range intermediates. This effect is profound at 1000 ppm addition, where the fastest oxidation of the lower range intermediates is observed. In terms of peak areas, Fig. 4d shows the lowest areas, thus demonstrating the effect of H_2O_2. The HPLC method used for the analysis of Iohexol was set at 254 nm, which is in-between the maximum absorbance of the central aromatic ring (Weast, 1985), and therefore, the detected intermediates have their central ring intact. Since H_2O_2 addition has caused lower detection in overall, it means that it actively contributes to the mineralization of the parent compound and the generated by-products, due to the non-selectivity of the HO• radicals.

In order to assess the extent of mineralization, further investigation was initiated, focusing in the degradation of the compound and the reduction of organic load in the bulk. The three tests assayed and presented in Fig. 5 are UV, UV/H_2O_2 and UV/H_2O_2/Fe^{2+} process. Enhancing the UV degradation process with H_2O_2 and then with Fe^{2+} and H_2O_2 inflicted a $t_{90\%}$ reduction of 40 and 50% respectively for the two aforementioned additions. Nevertheless, the addition of iron enhanced only the early stages of the treatment, as the time necessary for complete elimination was similar with the UV/H_2O_2 process alone.

Furthermore, the COD evolution shows a very similar behavior for UV photolysis and UV/H_2O_2 oxidation. Up to 30 min of treatment, the two processes are quasi-identical which means that there is transformation to more readily oxidized forms of carbon rather than actual degradation of the total carbon content. On the other hand, the presence of iron in the solution that enhances the hydroxyl radical generation demonstrates an immediate and constant rhythm of reduction. Most probably, the degradation

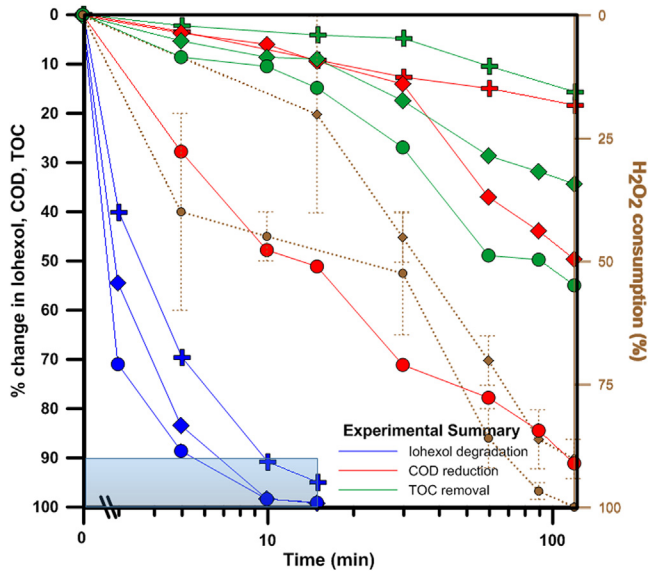

Fig. 5. Iohexol elimination by the UV-based AOPs. Iohexol degradation was followed by HPLC (blue trace), COD (red trace) and TOC decrease (green trace) during the following treatment methods: UV photolysis (trace: ✚), UV/H_2O_2 process (50 ppm H_2O_2, trace: ◆), and UV/H_2O_2/Fe^{2+} process (5 ppm Fe^{2+}, 50 ppm H_2O_2, trace: ●). H_2O_2 reduction: brown traces. A system employing 35-W UV-C lamps (instead of the 11-W ones of the previous parts, but otherwise identical) was used here. 100 ppm Iohexol was chosen as initial spiking. (For interpretation of the references to colour in this figure legend, the reader is referred to the web version of this article.)

pathway of the combined UV/H_2O_2/Fe^{2+} process has different steps than the oxidation process, such as enhanced side chains breakage instead of simple substitutions.

Finally, as far as the TOC removal is concerned, the compound confirms its highly recalcitrant behavior, with the three processes demonstrating similar and limited reduction for the first 15–20 min. After the total (parent) Iohexol removal, the TOC is further reduced, up to 30 and 55% for UV/H_2O_2 and UV/H_2O_2/Fe^{2+}, respectively. This TOC removal justifies experimentally for the first time so far in this investigation that extended treatment in presence of H_2O_2 and Fe^{2+} will eliminate the majority of the organic carbon present in the solution.

If we consider the Average Oxidation State as a normalized measure to assess the overall oxidation state of the solution (Bandara et al., 1997), we get (Equation (6)):

$$AOS = 4 \times \left(\frac{TOC - COD}{TOC}\right) \quad (6)$$

where COD and TOC values are expressed in mol O_2/L and mol C/L, respectively, and ranges from −4 (fully oxidizable, e.g. CH_4) to +4 for CO_2 (completely oxidized).

For each case, for time 0 to time 120 min:

A) UV AOS: from 0.1 to 0.25.
B) UV/H_2O_2 AOS: from 0.1 to 1.03.
C) UV/H_2O_2/Fe^{2+} AOS: from 0.1 to 3.24.

As it appears, for the same conditions, only with a moderate iron addition, the overall system did not leave residual H_2O_2, which strengthens the economic design of the system and secondly, the overall state of the system demonstrates an almost complete carbon elimination. Therefore, apart from the Iohexol removal, which is moderately enhanced, the intermediates can be effectively removed, which is often a common question when treating (recalcitrant) pharmaceuticals (Sarria et al., 2003; Malato et al., 2009).

What was made evident, is that the degradation process differs among the three processes. For this reason, the degradation products from the different treatment methods (after 5 min) were identified by HPLC-HR-MS analysis according to the corresponding spectral characteristics: mass spectra, accurate mass and characteristic fragmentation. Supplementary Tables S2.1 and S2.2 show the molecular formulas, double bond equivalent (DBE), theoretical and experimental masses along with mass accuracy (Δm) expressed in ppm.

In order to depict the differences, a synthetic representation of the intermediate products is shown in Fig. 6. For all the studied treatment methods, the degradation of Iohexol starts by scission of iodine from the aromatic ring and subsequent addition of −OH at iodo-sites, which results in single or double de-iodination, forming the phenolic products P1 and P6. Additionally, two more products were produced via direct attack of HO• on the side chain of Iohexol molecule (C1 and P3), with ketone formation and side-chain breakage, respectively. Identified products are in the agreement with some products identified by Jeong et al. (2010).

After P1, the degradation continues with HO• attack on side chains via oxidation, − OH addition, protonation and decarboxylation reactions, as seen in relevant works, (Jeong et al., 2010; Zhao et al., 2014; Tian et al., 2014), with minor differences between the treatments (different color arrows). Indeed, the influence of the UV irradiation is the main actor in the degradation process. However, degradation at P1, which also includes HO• attacks by treatment B and C (UV/H_2O_2 and UV/H_2O_2/Fe^{2+}) continues with the loss of a second iodine atom, resulting to product P6. At this point, the degradation with UV (treatment A) is finished. The biggest differences in the products appeared after P6 degradation, with four products identified for treatment B and three for treatment C. The degradation of the P6 product is a pathway that is based on UV exposure, as all processes, but proceeds further only in presence of H_2O_2 and/or Fe^{2+}. The structure of these by-products suggests that the degradation continues via the removal of the third iodine atom, plus further oxidation and decarboxylation of side chains. However, the appearance of unique and different products for treatments B and C imply that formation rate of HO• plays crucial role in all stages of the degradation process. Also, it is also noteworthy that in several pathways the formation of a non-ring hydroxylated derivative of Iohexol is derived from ring-hydroxylated TP of Iohexol, which is rare, but has occurred again in relevant literature (Csay et al., 2012; Jović et al., 2013).

Additionally, the use of Fe^{2+} and its affinity to the side chain structures, results to their higher substitution or breaking. From the products' structure, it could be concluded that the addition of iron is increasing the efficiency of the treatment, giving products with shorter side chains (products C4 and C5), and even nitrogen removal (product C4). The presence of hydroxyl radicals is responsible for their further degradation, as well as for the oxidation of the side chains removed. The MS analysis at 5 min corroborates with the HPLC results, which detection took place at 254 nm, indicating that the aromatic ring remains intact. Nevertheless, at 15 min, there is identified presence of products without iodine atoms, with the aromatic ring, but with degraded side chains. Finally, the absorbance spectra (see Supplementary Fig. S3) shifts significantly after 15 min of treatment, there are no exclusive UV pathways and mineralization initiates after this point, therefore we can conclude that the processes B and C involving HO• attacks and especially C, are the most efficient. The addition of iron is strongly recommended for efficient parent compound and by-product degradation.

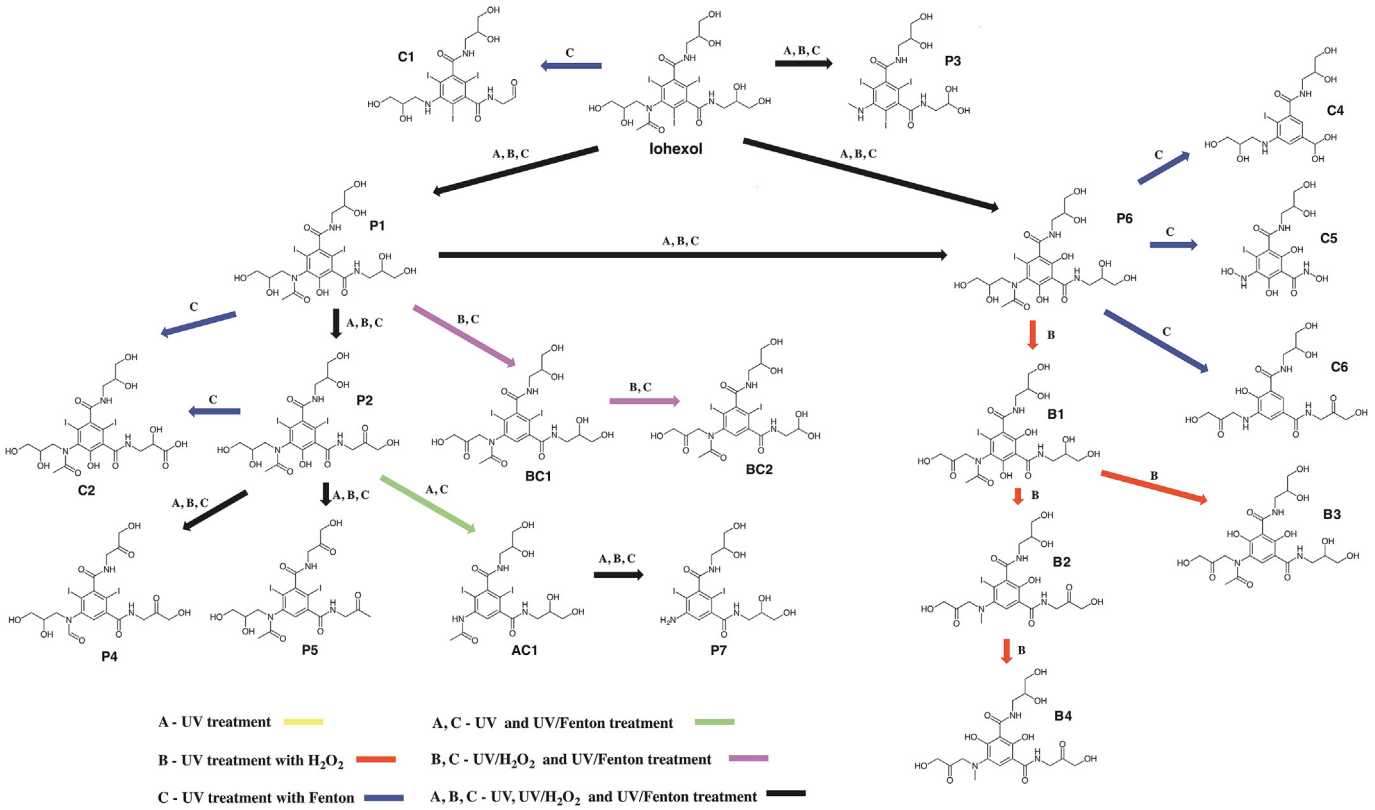

Fig. 6. Overall mechanistic degradation pathway of Iohexol treated by UV-based AOPs. Products common for all three treatments were marked with P, UV marked with A, for UV/H_2O_2 with B and for UV/H_2O_2/Fe^{2+} with C. Products common for A and C treatment were marked as AC, and accordingly, products common for B and C treatment were marked as BC.

4. Conclusions

Iodinated Contrast Media, such as the investigated Iohexol, can burden the environment with their presence for a relatively long time, due to their refractory nature. Since AOPs gained more attention over the last decades, the abilities of the synthetic UV/H_2O_2/Fe^{2+} process were assayed. To achieve efficient degradation and deep insight on the inactivation pathway, in the present work we assessed three approaches in degrading this drug, namely the operational parameter testing, the statistical optimization and the analytical chemical investigation.

As it appears, the dominant driving force in Iohexol degradation is the UV-C irradiation. The undertaken assays however, showed that the $t_{90\%}$, as a measure of comparison among the various experiments, can be moderately reduced if H_2O_2 and/or Fe^{2+} are added in the bulk. Also, depending on the matrix used, dilution was proven very effective in reducing organic matter and solids concentration, thus enhancing the removal of Iohexol.

The process was very well described by a quadratic model, which provided the best prediction of the kinetics constant for both wastewater and urine, and diluted or undiluted matrix. Also, a multiplicative model was produced, which sustained adequate accuracy while offering a simple formula. Additionally, the target of indicating the optimal operation regions for Iohexol degradation was achieved.

Finally, evidence for the main degradation actor and the evolution of the process, as well as the intermediates formed during the degradation of the parent compound were obtained. H_2O_2 and Fe, while macroscopically had a modest effect, their contribution in the mineralization is noteworthy. This is of high importance, as the ICM are notorious for their recalcitrance and their subsequent presence in the environment. Hence, although initially H_2O_2 and Fe^{2+} presence seem as an economic side-effect, our investigation suggests the optimization of their quantities and their addition to the UV process, which can effectively reduce the organic pollution in the subsequent matrices.

Acknowledgments

Stefanos Giannakis acknowledges the Swiss Agency for Development and Cooperation (SDC) and the Swiss National Foundation for the Research for Development Grant, for the funding through the project “Treatment of the hospital wastewaters in Côte d’Ivoire and in Colombia by advanced oxidation processes” (Project No. 146919).

Appendix A. Supplementary data

Supplementary data related to this article can be found at http://dx.doi.org/10.1016/j.jenvman.2016.07.004.

References

Bandara, J., Pulgarin, C., Peringer, P., Kiwi, J., 1997. Chemical (photo-activated) coupled biological homogeneous degradation of p-nitro-o-toluene-sulfonic acid in a flow reactor. J. Photochem. Photobiol. A Chem. 111 (1), 253–263.
Beach, H., 1971. Composition and Concentrative Properties of Human Urine. NASA Contractor Report. National Aeronautics and Space Administration, Washington, D. C. July 1971.
Borowska, E., Felis, E., Żabczyński, S., 2014. Degradation of iodinated contrast media in aquatic environment by means of UV, UV/TiO2 process, and by activated sludge. Water, Air, & Soil Pollut. 226 (5), 1–12.
Canonica, S., Meunier, L., Von Gunten, U., 2008. Phototransformation of selected pharmaceuticals during UV treatment of drinking water. Water Res. 42 (1),

121–128.
Chèvre, N., 2014. Pharmaceuticals in surface waters: sources, behavior, ecological risk, and possible solutions. Case study of Lake Geneva, Switzerland. Wiley Interdiscip. Rev. Water 1 (1), 69–86. http://dx.doi.org/10.1002/wat2.1006.
Csay, T., Rácz, G., Takács, E., Wojnárovits, L., 2012. Radiation induced degradation of pharmaceutical residues in water: chloramphenicol. Radiat. Phys. Chem. 81 (9), 1489–1494.
Davis, B., Saltman, P., Benson, S., 1962. The stability constants of the iron-transferrin complex. Biochem. Biophy. Res. Commun. 8 (1–2), 56–60. http://dx.doi.org/10.1016/0006-291X(62)90235-8.
De la Cruz, N., Esquius, L., Grandjean, D., Magnet, A., Tungler, A., de Alencastro, L.F., Pulgarin, C., 2013. Degradation of emergent contaminants by UV, UV/H2O2 and neutral photo-Fenton at pilot scale in a domestic wastewater treatment plant. Water Res. 47 (15), 5836–5845. http://dx.doi.org/10.1016/j.watres.2013.07.005.
De la Cruz, N., Gimenez, J., Esplugas, S., Grandjean, D., de Alencastro, L.F., Pulgarin, C., 2012. Degradation of 32 emergent contaminants by UV and neutral photo-fenton in domestic wastewater effluent previously treated by activated sludge. Water Res. 46 (6), 1947–1957. http://dx.doi.org/10.1016/j.watres.2012.01.014.
Doll, T.E., Frimmel, F.H., 2004. Kinetic study of photocatalytic degradation of carbamazepine, clofibric acid, iomeprol and iopromide assisted by different TiO 2 materials—determination of intermediates and reaction pathways. Water Res. 38 (4), 955–964.
Giannakis, S., Gamarra Vives, F.A., Grandjean, D., Magnet, A., De Alencastro, L.F., Pulgarin, C., 2015. Effect of advanced oxidation processes on the micropollutants and the effluent organic matter contained in municipal wastewater previously treated by three different secondary methods. Water Res. 84, 295–306. http://dx.doi.org/10.1016/j.watres.2015.07.030.
Guo, H.-G., Gao, N.-Y., Chu, W.-H., Li, L., Zhang, Y.-J., Gu, J.-S., Gu, Y.-L., 2013. Photochemical degradation of ciprofloxacin in UV and UV/H2O2 process: kinetics, parameters, and products. Environ. Sci. Pollut. Res. 20 (5), 3202–3213. http://dx.doi.org/10.1007/s11356-012-1229-x.
Haiß, A., Kümmerer, K., 2006. Biodegradability of the X-ray contrast compound diatrizoic acid, identification of aerobic degradation products and effects against sewage sludge micro-organisms. Chemosphere 62 (2), 294–302.
Herrera, F., Pulgarin, C., Nadtochenko, V., Kiwi, J., 1998. Accelerated photo-oxidation of concentrated p-coumaric acid in homogeneous solution. Mechanistic studies, intermediates and precursors formed in the dark. Appl. Catal. B Environ. 17 (1–2), 141–156. http://dx.doi.org/10.1016/S0926-3373(98)00008-3.
Jeong, J., Jung, J., Cooper, W.J., Song, W., 2010. Degradation mechanisms and kinetic studies for the treatment of X-ray contrast media compounds by advanced oxidation/reduction processes. Water Res. 44 (15), 4391–4398.
Jović, M., Manojlović, D., Stanković, D., Dojčinović, B., Obradović, B., Gašić, U., Roglić, G., 2013. Degradation of triketone herbicides, mesotrione and sulcotrione, using advanced oxidation processes. J. Hazard Mater 260, 1092–1099.
Luo, Y., Guo, W., Ngo, H.H., Nghiem, L.D., Hai, F.I., Zhang, J., Wang, X.C., 2014. A review on the occurrence of micropollutants in the aquatic environment and their fate and removal during wastewater treatment. Sci. Total Environ. 473–474, 619–641. http://dx.doi.org/10.1016/j.scitotenv.2013.12.065.
Mack, J., Bolton, J.R., 1999. Photochemistry of nitrite and nitrate in aqueous solution: a review. J. Photochem. Photobiol. A Chem. 128 (1–3), 1–13. http://dx.doi.org/10.1016/S1010-6030(99)00155-0.
Malato, S., Fernández-Ibáñez, P., Maldonado, M.I., Blanco, J., Gernjak, W., 2009. Decontamination and disinfection of water by solar photocatalysis: recent overview and trends. Catal. Today 147 (1), 1–59. http://dx.doi.org/10.1016/j.cattod.2009.06.018.
Margot, J., Kienle, C., Magnet, A., Weil, M., Rossi, L., De Alencastro, L.F., Schärer, M., 2013. Treatment of micropollutants in municipal wastewater: ozone or powdered activated carbon? Sci. Total Environ. 461, 480–498.
Margot, J., Magnet, A., Thonney, D., Chèvre, N., Alencastro, D., Felippe, L., Rossi, L., 2011. Traitement des micropolluants dans les eaux usées-Rapport final sur les essais pilotes à la STEP de Vidy (Lausanne) (Ville de Lausanne).
McArdell, C.S., Kovalova, L., 2010. Input and Elimination of Pharmaceuticals and Disinfectants from Hospital Wastewater. EAWAG.
Ort, C., Lawrence, M.G., Reungoat, J., Eaglesham, G., Carter, S., Keller, J., 2010. Determining the fraction of pharmaceutical residues in wastewater originating from a hospital. Water Res. 44 (2), 605–615.
Papoutsakis, S., Afshari, Z., Malato, S., Pulgarin, C., 2015a. Elimination of the iodinated contrast agent iohexol in water, wastewater and urine matrices by application of photo-fenton and ultrasound advanced oxidation processes. J. Environ. Chem. Eng. 3 (3), 2002–2009.
Papoutsakis, S., Miralles-Cuevas, S., Oller, I., Sanchez, J.G., Pulgarin, C., Malato, S., 2015b. Microcontaminant degradation in municipal wastewater treatment plant secondary effluent by EDDS assisted photo-Fenton at near-neutral pH: an experimental design approach. Catal. Today 252, 61–69.
Pereira, V.J., Linden, K.G., Weinberg, H.S., 2007. Evaluation of UV irradiation for photolytic and oxidative degradation of pharmaceutical compounds in water. Water Res. 41 (19), 4413–4423.
Pérez, S., Barceló, D., 2007. Fate and occurrence of X-ray contrast media in the environment. Anal. Bioanal. Chem. 387 (4), 1235–1246.
Pills project, (2012). http://www.pills-project.eu/, (accessed 15.2.16.).
Pulgarin, C., Kiwi, J., 1996. Overview on photocatalytic and electrocatalytic pretreatment of industrial non-biodegradable pollutants and pesticides. CHIMIA Int. J. Chem. 50 (3), 50–55.
Putschew, A., Wischnack, S., Jekel, M., 2000. Occurrence of triiodinated X-ray contrast agents in the aquatic environment. Sci. Total Environ. 255 (1), 129–134.
Sarria, V., Kenfack, S., Guillod, O., Pulgarin, C., 2003. An innovative coupled solar-biological system at field pilot scale for the treatment of biorecalcitrant pollutants. J. Photochem. Photobiol. A Chem. 159 (1), 89–99.
Seitz, W., Jiang, J.-Q., Schulz, W., Weber, W.H., Maier, D., Maier, M., 2008. Formation of oxidation by-products of the iodinated X-ray contrast medium iomeprol during ozonation. Chemosphere 70 (7), 1238–1246.
Sharpless, C.M., Linden, K.G., 2001. UV photolysis of nitrate: effects of natural organic matter and dissolved inorganic carbon and implications for UV water disinfection. Environ. Sci. Technol. 35 (14), 2949–2955. http://dx.doi.org/10.1021/es002043l.
Sprehe, M., Geissen, S.U., 2000. Verfahrensauswahl zur AOX eliminierung im krankenhausabwasserbereich. In: Halogenorganische verbindungen, vol. 18. Herausgeber ATV-DVWK, pp. 257–268. ATV-DVWK Schriftenreihe.
Sugihara, M.N., Moeller, D., Paul, T., Strathmann, T.J., 2013. TiO2-photocatalyzed transformation of the recalcitrant X-ray contrast agent diatrizoate. Appl. Catal. B Environ. 129, 114–122.
Ternes, T.A., Hirsch, R., 2000. Occurrence and behavior of X-ray contrast media in sewage facilities and the aquatic environment. Environ. Sci. Technol. 34 (13), 2741–2748.
Tian, F.-X., Xu, B., Lin, Y.-L., Hu, C.-Y., Zhang, T.-Y., Gao, N.-Y., 2014. Photodegradation kinetics of iopamidol by UV irradiation and enhanced formation of iodinated disinfection by-products in sequential oxidation processes. Water Res. 58, 198–208. http://dx.doi.org/10.1016/j.watres.2014.03.069.
Verlicchi, P., Al Aukidy, M., Galletti, A., Petrovic, M., Barcelo, D., 2012. Hospital effluent: investigation of the concentrations and distribution of pharmaceuticals and environmental risk assessment. Sci. Total Environ. 430, 109–118. http://dx.doi.org/10.1016/j.scitotenv.2012.04.055.
Viollier, E., Inglett, P.W., Hunter, K., Roychoudhury, A.N., Van Cappellen, P., 2000. The ferrozine method revisited: Fe(II)/Fe(III) determination in natural waters. Appl. Geochem. 15 (6), 785–790. http://dx.doi.org/10.1016/S0883-2927(99)00097-9.
Vione, D., Minella, M., Maurino, V., Minero, C., 2014. Indirect photochemistry in sunlit surface waters: photoinduced production of reactive transient species. Chem. – A Eur. J. 20 (34), 10590–10606. http://dx.doi.org/10.1002/chem.201400413.
Weast, R.C., 1985. Handbook of Data on Organic Compounds.
Weissbrodt, D., Kovalova, L., Ort, C., Pazhepurackel, V., Moser, R., Hollender, J., …, McArdell, C.S., 2009. Mass flows of X-ray contrast media and cytostatics in hospital wastewater. Environ. Sci. Technol. 43 (13), 4810–4817. http://dx.doi.org/10.1021/es8036725.
Wu, C., Linden, K.G., 2010. Phototransformation of selected organophosphorus pesticides: roles of hydroxyl and carbonate radicals. Water Res. 44 (12), 3585–3594. http://dx.doi.org/10.1016/j.watres.2010.04.011.
Zhao, C., Arroyo-Mora, L.E., DeCaprio, A.P., Sharma, V.K., Dionysiou, D.D., O'Shea, K.E., 2014. Reductive and oxidative degradation of iopamidol, iodinated X-ray contrast media, by Fe (III)-oxalate under UV and visible light treatment. Water Res. 67, 144–153.